

See discussions, stats, and author profiles for this publication at: <https://www.researchgate.net/publication/267742362>

Rapid, Selective, and Ultrasensitive Fluorimetric Analysis of Mercury and Copper Levels in Blood Using Bimetallic Gold–Silver Nanoclusters with “Silver Effect”–Enhanced Red Fluores...

ARTICLE *in* ANALYTICAL CHEMISTRY · OCTOBER 2014

Impact Factor: 5.64 · DOI: 10.1021/ac503102g · Source: PubMed

CITATIONS

10

READS

20

7 AUTHORS, INCLUDING:



Hua Wang

Qufu Normal University

164 PUBLICATIONS 1,852 CITATIONS

SEE PROFILE

Rapid, Selective, and Ultrasensitive Fluorimetric Analysis of Mercury and Copper Levels in Blood Using Bimetallic Gold–Silver Nanoclusters with “Silver Effect”-Enhanced Red Fluorescence

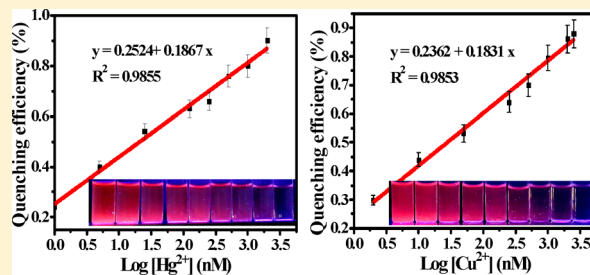
Ning Zhang,[†] Yanmei Si,[†] Zongzhao Sun,[†] Lijun Chen,[‡] Rui Li,[†] Yuchun Qiao,[†] and Hua Wang^{*,†}

[†]Shandong Province Key Laboratory of Life-Organic Analysis, School of Chemistry and Chemical Engineering, Qufu Normal University, Qufu City, Shandong 273165, P. R. China

[‡]Hospital of University, Qufu Normal University, Qufu City, Shandong 273165, P. R. China

S Supporting Information

ABSTRACT: Bimetallic alloying gold–silver nanoclusters (Au-AgNCs) have been synthesized by a one-pot biomimetic synthesis route at a vital molar ratio of Au/Ag precursors in the protein matrix. Unexpectedly, the prepared Au-AgNCs could exhibit dramatically enhanced red fluorescence, which is about 6.5-fold and 4.7-fold higher than that of common AuNCs and core–shell Au@AgNCs, respectively. A rapid, selective, and ultrasensitive fluorimetric method has thereby been developed using Au-AgNCs as fluorescent probes toward the separate detections of Hg²⁺ and Cu²⁺ ions in blood. The interactions of Au-AgNCs with Hg²⁺ and Cu²⁺ ions were systematically characterized by microscopy imaging, UV-vis, and fluorescence measurements. It is demonstrated that the “silver effect” gives the Au-AgNCs probes not only greatly enhanced red fluorescence but also the strong capacity to specifically sense Cu²⁺ ions in addition to improved response to Hg²⁺ ions. Moreover, aided by a Cu²⁺ chelating agent, exclusive detection of Hg²⁺ ions could also be expected with the coexistence of a high level of Cu²⁺ ions, as well as reversible Cu²⁺ analysis by restoring the fluorescence of Au-AgNCs. Additionally, Au-AgNCs with strong red fluorescence could facilitate fluorimetric analysis with minimal interference from blood backgrounds. Such an Au-AgNCs-based fluorimetric method can allow for the selective analysis of Hg²⁺ and Cu²⁺ ions down to 0.30 nM and 0.60 nM in blood, respectively, promising a novel detection method to be applied in the clinical laboratory.



Heavy metal pollution has received increasing concern throughout the world because of adverse effects on the environment and especially human health.¹ Mercury is one of the most toxic heavy metals that extensively exists in air, water, soil, and food.² The accumulation of mercury in the human body can severely damage the digestive, excretory, and even central nervous system, resulting in a variety of serious diseases such as tremors, deafness, arthritis, loss of muscle coordination, sensation, and memory, and motor disorders. Moreover, copper ions play vital roles in many fundamental biological processes such as metabolism, growth, and immune system development.³ Clinical studies indicate that copper deficiency may cause various diseases; however, a high copper concentration in tissues can also bring deleterious effects. For example, long-term exposure to high levels of copper ions can lead to cellular toxicity⁴ and liver and kidney damage.⁵ Therefore, it is of great interest to develop a simple, rapid, and highly sensitive detection method for mercury and copper ions especially in human body fluids (i.e., blood).

To date, many analysis technologies have been developed to detect heavy metal ions including Cu²⁺ and Hg²⁺ ions, such as atomic absorption spectrometry,⁶ plasma mass spectrometry,⁷ electrochemical sensing methods,⁸ colorimetric assays,^{9,10} and fluorescence detection methods.¹¹ Among these analysis

methods, fluorescent detection methods are ideal due to distinct advantages such as high sensitivity, simplicity, and short response time. Traditionally, organic dyes are widely utilized as fluorescent probes for the detection of heavy metal ions.^{12,13} However, organic dyes might suffer from small Stokes shift, short lifetime, and poor photostability. Alternatively, considerable attention has been drawn to the preparation and applications of fluorescent inorganic nanomaterials due to their intense luminescence, high photochemical stability, and wide spectral line. As the most typical example, fluorescent quantum dots (QDs) ((i.e., CdS, CdSe, and ZnS) have been introduced for fluorescent detection strategies.^{14,15} For example, CdS QDs were applied as fluorescent probes for the detection of low-level mercury(II).¹⁵ These QD methods are sensitive, but they might involve harsh and complicated synthesis procedures for the detection of environmentally toxic metals.

Recent years have witnessed the rapid development of fluorescent noble metal nanomaterials, widely known as gold nanoclusters (AuNCs) and silver nanoclusters (AgNCs), which

Received: August 19, 2014

Accepted: October 28, 2014

Published: October 28, 2014

have been synthesized by using environmentally benign templates such as peptides, gelatin, proteins, and DNA.^{10,16–18} These fluorescent nanoclusters exhibit ultrasmall size, low toxicity, and strong fluorescence, so they have been extensively applied in biolabeling,¹⁹ bioimaging,²⁰ catalysis,²¹ and ion sensing.^{2,18,22,23} Moreover, increasing efforts have been recently devoted to the synthesis of bimetallic Au/Ag nanomaterials, aiming to combine their synergistic effects to achieve more attractive advantages over the monometallic ones for electronic, optical, and catalytic performance.^{24–26} For example, Shi et al. discovered a long-overlooked “silver effect” in gold catalysis, which gives bimetallic Au/Ag nanoparticles catalytic activities much higher than those of Au nanoparticles alone.²⁶ Also, some luminescent bimetallic Au/AgNCs have been fabricated and/or applied by the introduction of silver to change the luminescence of AuNCs.^{22,23,27–29} For example, highly luminescent bimetallic Au/AgNCs were synthesized in Zhu's group using a one-pot sonochemical synthesis procedure.²³ Gui and co-workers prepared core–shell Au/AgNCs for the fluorescent detection of cysteine and homocysteine.²⁹ Pal's group also synthesized giant fluorescent Au(I)@Ag clusters by a two-step route for sensing mercury(II) ions.³⁰ Although the significant effects of the silver composition on the luminescence intensities of the bimetallic Au/AgNCs have been recognized,^{22,28} two contrary observations were reported for the roles that the “silver effect” could play in influencing the luminescence of bimetallic Au/AgNCs, an increase²² and a decrease,²⁸ in the fluorescence intensity compared with that of AuNCs. Additionally, the synergistic responses of bimetallic Au/AgNCs to Hg²⁺ and Cu²⁺ ions have hardly been studied systematically toward the analysis of heavy metal ions, despite the separate interactions of AuNCs with Hg²⁺ ions and AgNCs with Cu²⁺ ions that have been explored.^{22,31}

In the present work, inspired by the “silver effect” in enhancing gold catalysis, we sought to prepare bimetallic Au/AgNCs with strong fluorescence to serve as fluorescent probes for a new fluorimetric method. Initially, bimetallic core–shell Au@AgNCs were prepared by the common two-step biomimetic route above, achieving a small increase in fluorescence intensity compared with that of AuNCs. Alternatively, bimetallic alloying Au-AgNCs were synthesized using a new facile one-pot biomimetic route by adjusting the molar ratios of Au/Ag precursors in the protein matrix. Unexpectedly, dramatically enhanced red fluorescence was obtained at vital molar ratios of Au/Ag precursors (i.e., 25/6). Importantly, when the alloying Au-AgNCs were employed to probe 15 kinds of common metal ions, only Hg²⁺ and Cu²⁺ ions could share a significant fluorescence quenching of Au-AgNCs. Moreover, the interaction mechanism and sensing performance of alloying Au-AgNCs for Hg²⁺ and Cu²⁺ ions were systematically investigated by using techniques such as high-resolution transmission electron microscopy (HR-TEM) and optical spectroscopy. A rapid, selective, and ultrasensitive fluorimetric method has thus been developed for analyzing Hg²⁺ and Cu²⁺ ions in blood. It was demonstrated that the “silver effect” in the alloying Au-AgNCs gave the fluorescent probes not only greatly enhanced red fluorescence compared with that of AuNCs but also the new ability to specifically sense Cu²⁺ ions and to improve the detection of Hg²⁺ ions. The feasibility of the developed fluorimetric strategy for the detections of Hg²⁺ and Cu²⁺ ions in blood was demonstrated with high sensitivity and selectivity.

EXPERIMENTAL SECTION

Reagents and Apparatus (see Supporting Information). *Synthesis of Bimetallic Alloying Au-AgNCs.* Bimetallic alloying Au-AgNCs were prepared using bovine serum albumin (BSA) as the protein stabilization and reduction agent at different molar ratios of HAuCl₄ and AgNO₃. An aliquot of HAuCl₄ solution (2.0 mL, 10 mM) was added to the BSA solution (2.0 mL, 0.75 mM). Then, AgNO₃ solutions (0.80 mL) of different concentrations (2.0, 4.0, 6.0, 8.0, and 10 mM, 37 °C) were separately added under vigorous stirring for 5.0 min. Afterward, NaOH solution (0.20 mL, 1.0 M) was introduced and incubated at 37 °C for 12 h. Finally, the resulting solution was dialyzed in water for 48 h. The so-obtained Au-AgNCs were stored at 4 °C. Notably, the synthesis of alloying Au-AgNCs at the optimized Au/Ag molar ratio of 25/6 was conducted using 4.0 mM HAuCl₄, 0.96 mM AgNO₃, and 0.30 mM BSA in the final solution. In addition, core–shell Au@AgNCs were prepared accordingly by using the two-step synthetic route.²²

Fluorimetric Detections of Metal Ions. Selective detections for Hg²⁺ and Cu²⁺ ions in water were conducted by basically following a similar procedure. First, an aliquot of Au-AgNCs (0.417 mM) was separately added to a Hg²⁺ solution at different concentrations (0, 0.20, 1.0, 5.0, 25, 125, 625, 1250, 2500 nM). The mixtures were incubated at room temperature for 5 min and measured by a fluorescence spectrometer. Second, by following the same analysis procedure, Cu²⁺ ions at different concentrations in water (0, 0.50, 1.0, 5.0, 25, 125, 625, 1250, 2500 nM) were analyzed. Third, exclusive detections of Hg²⁺ ions at different concentrations (0, 0.50, 2.5, 10, 50, 250, 1000, 2000, 3000 nM) were performed at the fixed concentrations of Cu²⁺ (500 nM) and EDTA (600 nM). Fourth, control tests for 1.0 μM metal ion (Ag⁺, Na⁺, Hg²⁺, Pb²⁺, Fe²⁺, Fe³⁺, Mg²⁺, Cu²⁺, Ca²⁺, Zn²⁺, Ni²⁺, Ba²⁺, Cr³⁺, K⁺, Co²⁺) were conducted accordingly. Fifth, by following the same procedures above, the developed fluorimetric assays were applied to detect different concentrations of Hg²⁺ ions (1.0, 5.0, 25, 125, 250, 500, 1000, 2000 nM) and Cu²⁺ ions (2.0, 10, 50, 250, 500, 1000, 2000, 2500 nM), which were separately spiked in fresh blood samples. Herein, the quenching efficiencies of Au-AgNCs by metal ions were calculated according to the following equation: quenching efficiencies = $(F_0 - F)/F_0$, where F_0 and F refer to the fluorescence intensities of Au-AgNCs (λ_{em} 620 nm) in the absence and presence of metal ions, respectively. Additionally, the developed method was applied to probe Hg²⁺ and Cu²⁺ ions in real blood samples, compared with the classic inductively coupled plasma-mass spectrometry (ICP-MS) method used in the clinical laboratory.

RESULTS AND DISCUSSION

Synthesis and Characterization of Fluorescent Bimetallic Au-AgNCs. It is well recognized that the “silver effect” could significantly influence gold catalysis²⁶ and luminescence performance of AuNCs by forming bimetallic Au/AgNCs.^{22,28} According to the common two-step biomimetic route documented,²² bimetallic core–shell Au@AgNCs were initially prepared but only showed a small increase in fluorescence intensity compared to that for AuNCs. Alternatively, bimetallic alloying Au-AgNCs were synthesized using a new facile one-pot biomimetic route by adjusting the molar ratios of Au/Ag precursors in the protein matrix. Unexpectedly, dramatically

enhanced fluorescence was obtained for alloying Au-AgNCs compared to AuNCs and core–shell Au@AgNCs but at a vital molar ratio of Au/Ag precursors (i.e., 25/6) in the protein matrix. Figure 1 shows the morphological HR-TEM images of

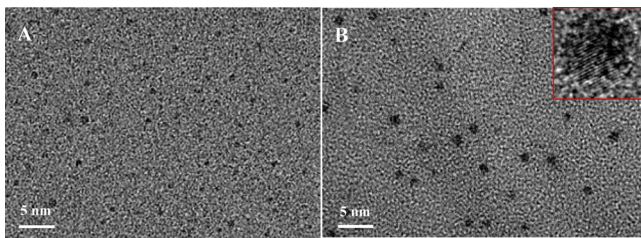


Figure 1. HR-TEM images of (A) AuNCs and (B) Au-AgNCs (insert: the amplified image), where the bimetallic alloys were synthesized at a Au/Ag molar ratio of 25/6.

the resulting Au-AgNCs, using AuNCs as a comparison. The size of Au-AgNCs (Figure 1B) is much larger than that of AuNCs (Figure 1A), the average hydrodynamic diameters being about 4.5 and 2.0 nm, respectively, calculated by dynamic light scattering (DLS) (Figure S1, Supporting Information). Additionally, as shown in the amplified HR-TEM image (Figure 1B, inset), there is no obvious lattice mismatch or core–shell structure observed for Au-AgNCs, implying that they might be formed in bimetallic alloys. For further confirmation, energy dispersive spectroscopy (EDS) and elemental mapping measurements were performed for an individual giant cluster of Au-AgNCs in the bulk protein matrix (Figure S2A,B, Supporting Information). Au-AgNCs were composed of Au and Ag elements uniformly dispersed in a discretely mixed way (Figure S2B), resulting in a spatially resolved distribution of alloying Au-AgNCs. Furthermore, X-ray diffraction (XRD) analysis revealed that the sharp peaks at 31.74° and 45.5° could correspond to lattice planes (111) and (200) of Au-AgNCs, respectively (Figure S2C). The XRD peaks of Au-AgNCs separately deviate from the corresponding normalized peaks of 38.1° and 44.4°,^{32,33} indicating again the formation of alloying Au-AgNCs.

Moreover, the oxidation states of Au and Ag in Au-AgNCs were determined by X-ray photoelectron spectroscopy (XPS)

(Figure S3A,B). The binding energies (Au 4f_{7/2}, 84.1 eV; Au 4f_{5/2}, 87.6 eV) confirm a dominant Au(0) metallic state in Au-AgNCs (Figure S3A, Supporting Information). Meanwhile, the Ag 3d spectrum indicates that the binding energies of 367.8 eV (Ag 3d_{5/2}) and 374.2 eV (Ag 3d_{3/2}) could be assigned to be Ag(I) and Ag(0) in Au-AgNCs, respectively (Figure S3B).^{28,32} Accordingly, the alloying Au-AgNCs could consist of Au(0) and Ag(I)/Ag(0), in contrast to the core–shell Au@AgNCs with Au(I) and Ag(0) as reported elsewhere.³⁰ Furthermore, a peak at 163.3 eV (Figure S3C) could support the involvement of the S 2p in the Au–S bonding,²⁸ in which the S element could come from some specific side chains of the protein scaffold of Au-AgNCs, i.e., 35 cysteine residues of BSA.¹⁷ The main XPS spectrum for the protein-stabilized Au-AgNCs is shown in Figure S3D. Accordingly, bimetallic Au-AgNCs might be formed in the protein scaffold mostly anchoring at their S-containing exterior and interior via metal–S binding. On the basis of the experimental evidence above and referring to the documents,^{17,23,28,33} the formation process for bimetallic alloying Ag-AuNCs is proposed as follows. AuCl₄⁻ and Ag⁺ ions were first reduced by the reductive components of the protein scaffold, i.e., 21 tyrosines in BSA,¹⁷ causing Au and Ag atoms to form the nuclei of the bimetallic system. Because Au could present a relatively faster nucleation rate than Ag,³³ the previously formed Au NCs might in turn catalyze the deposition of Ag NCs, which is a well-known phenomenon. The codeposition of Au and Ag NCs could thus occur, leading to the formation of alloying Au-AgNCs that would grow to their final sizes in the protein matrix.

The silver composition-dependent fluorescence intensities of alloying Au-AgNCs were compared to those of AuNCs and core–shell Au@AgNCs, which were separately prepared using the same gold concentration and/or varying silver concentrations (Figure 2A). Both bimetallic Au-AgNCs and Au@AgNCs displayed luminescence higher than that of AuNCs, indicating the significant effects of the silver component on the luminescence enhancement issues. Particularly, alloying Au-AgNCs could present fluorescence much stronger than that of core–shell Au@AgNCs, although they were prepared with the same dosages of Au and Ag precursors. Moreover, the maximum fluorescence of alloying Au-AgNCs was obtained at 6.0 mM Ag⁺ precursor, and the fluorescence spectra are shown

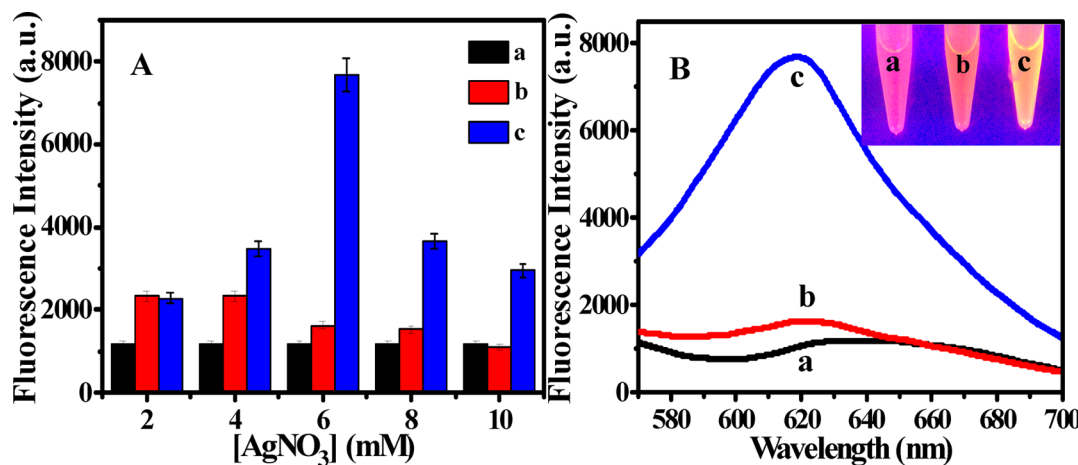


Figure 2. (A) Silver composition-dependent fluorescence intensities ($\lambda_{\text{ex}} = 370 \text{ nm}$) of (a) AuNCs, (b) Au@AgNCs, and (c) Au-AgNCs synthesized using 10 mM HAuCl₄ and different AgNO₃ concentrations (2.0, 4.0, 6.0, 8.0, and 10 mM). (B) The fluorescence spectra (insert: photographs under UV light) of (a) AuNCs, (b) Au@AgNCs, and (c) Au-AgNCs solutions. The bimetallic products were synthesized at a Au/Ag molar ratio of 25/6.

in Figure S4, Supporting Information. A further increase in Ag^+ concentration might lead to a decrease in fluorescence intensity. Accordingly, alloying Au-AgNCs could be obtained with the strongest fluorescence at a vital Au/Ag molar ratio of 25/6 (i.e., 4.0 mM HAuCl₄ and 0.96 mM AgNO₃ in the final solution). Herein, because the fluorescence of Au-AgNCs came from the Au emission, it could be enhanced by an appropriate Ag amount via the “silver effect”. Yet, it might be diminished by excessive Ag formation, especially when an Au-catalyzed silver deposition was involved as mentioned above.

Furthermore, the unique optical properties of the obtained Au-AgNCs were characterized by fluorescence spectroscopy (Figure 2B). The fluorescent emission of alloying Au-AgNCs could peak at about 620 nm, which is a small blue shift relative to AuNCs of 635 nm. More importantly, the maximum fluorescence intensity of alloying Au-AgNCs could be about 6.5-fold and 4.7-fold higher than that of AuNCs and Au@AgNCs, respectively. The corresponding photographs also indicate the “silver effect” in endowing Au-AgNCs the most luminescence (Figure 2B, insert). The quantum yield of alloying Au-AgNCs was measured to be about 10.5% using quinine sulfate as the reference, which is higher than that of AuNCs (about 6.0%). Also, Figure S5 (Supporting Information) shows the comparison of UV-vis absorption spectra among AuNCs, Au@AgNCs, and alloying Ag-AuNCs, with different shades of brown in visible light (insert). Alloying Au-AgNCs could present the strongest protein absorbance, although they were formed in the same concentration of protein matrix (0.30 mM BSA). Moreover, the UV-vis absorption spectra showed no obvious surface plasmon resonance over the gold or silver absorbance range, presumably due to alloying Au-AgNCs being formed in the bulky protein matrix,¹⁷ showing only a small fraction of the overall NC population.

Sensing Responses of the Au-AgNCs-Based Fluorimetry to Different Metal Ions. It is well established that Hg²⁺ ions and Cu²⁺ ions can have special interactions with Au⁺ on AuNCs and Ag⁺ around AgNCs, respectively.^{22,31} Accordingly, bimetallic alloying Au-AgNCs would be employed as the fluorescent probes to develop a new fluorimetry for sensing Hg²⁺ and Cu²⁺ ions. To explore the sensing selectivity, the developed fluorimetry was first used to comparably probe 15 kinds of common metal ions (1.0 μM), including Ag⁺, Na⁺, Hg²⁺, Pb²⁺, Fe²⁺, Fe³⁺, Mg²⁺, Cu²⁺, Ca²⁺, Zn²⁺, Ni²⁺, Ba²⁺, Cr³⁺, K⁺, Co²⁺ (Figure 3). As expected, only Cu²⁺ and Hg²⁺ ions could trigger the immediate and significant quenching of the

fluorescence of bimetallic Au-AgNCs, as shown in their corresponding photographs (Figure 3, insert). Obviously, Au-AgNCs could serve as robust fluorescent probes for the selective detections of Cu²⁺ and Hg²⁺ ions. Yet, the addition of Ag⁺ ions could also cause a small quenching effect on the fluorescence of Au-AgNCs to some extent. Such a phenomenon might meaningfully confirm the evidence aforementioned in the synthesis procedure of bimetallic Au-AgNCs, where Au-AgNCs were prepared with maximum fluorescence at a vital molar ratio of Au/Ag precursors. Therefore, the “silver effect”, herein, could not only greatly enhance the fluorescence of Au-AgNCs probes but could also endow them the specific ability for sensing Cu²⁺ ions in addition to Hg²⁺ ions.

Sensing Performances and Possible Mechanism of the Au-AgNCs-Based Fluorimetry for Hg²⁺ and Cu²⁺ Ions. The sensing performances of the Au-AgNCs-based fluorimetric method for Cu²⁺ and Hg²⁺ ions were studied separately by the fluorescence and UV-vis spectra (Figure 4). As shown in Figure 4A, bimetallic Au-AgNCs displayed strong red fluorescence at 620 nm (Figure 4A(a)). When Cu²⁺ and Hg²⁺ ions were separately introduced, the fluorescence of Au-AgNCs could be quenched dramatically (Figure 4A(b,d)), indicating the feasibility of separate detections for Cu²⁺ and Hg²⁺ ions. Moreover, the possibilities for exclusive Hg²⁺ detection and the reversibility of the Cu²⁺ analysis were investigated by adding the Cu²⁺ chelating reagent EDTA into the mixtures of Au-AgNCs separately with Cu²⁺ and Hg²⁺ ions. The addition of adequate EDTA could chelate Cu²⁺ ions to restore the fluorescence intensity of Au-AgNCs to 92% of its original value (Figure 4A(c)), while few effects were observed for the ones with Hg²⁺ ions (Figure 4A(e)). The above phenomena are also demonstrated by the photographs of their corresponding products (Figure 4A, insert). Therefore, the developed fluorimetric approach could facilitate the exclusive detection of Hg²⁺ in the presence of a high level of Cu²⁺ ions by using EDTA. Furthermore, Figure 4B shows the UV-vis spectra recorded for Au-AgNCs separately with Cu²⁺ and Hg²⁺ ions, including those after the addition of EDTA. The protein absorbance values of protein-stabilized Au-AgNCs (Figure 4B(a)) decreased after the exposure to Cu²⁺ ions (Figure 4B(b)) and Hg²⁺ ions (Figure 4B(d)). Also, the addition of EDTA to the mixture of Au-AgNCs with Cu²⁺ ions could restore the UV-vis absorbance of Au-AgNCs approximately to the original level (Figure 4B(c)), much higher than that of the ones with Hg²⁺ ions (Figure 4B(e)). Such an experimental phenomenon may imply that different interactions could occur among the protein scaffolds with Cu²⁺ and Hg²⁺ ions.

Figure 5 describes the morphological studies by TEM imaging for the bimetallic Au-AgNCs separately with Cu²⁺ or Hg²⁺ ions including the introduction of EDTA, in which their corresponding fluorescence changes were monitored alternatively by fluorescence microscopy (insert). No significant changes in the size and morphology were observed for Au-AgNCs with Hg²⁺ ions before (Figure 5A) and after the addition of EDTA (Figure 5B), which are also well consistent with that of native Au-AgNCs shown in Figure 1B. Nevertheless, fluorescence microscopy reveals that fluorescence quenching could occur for Au-AgNCs with Hg²⁺ ions (Figure 5A, insert), and the addition of EDTA could not restore the fluorescence (Figure 5B, insert). In contrast, the introduction of Cu²⁺ ions could apparently cause the aggregation of the protein scaffold with Au-AgNCs (Figure 5C), in addition to the fluorescence quenching (insert). More interestingly, Figure 5D

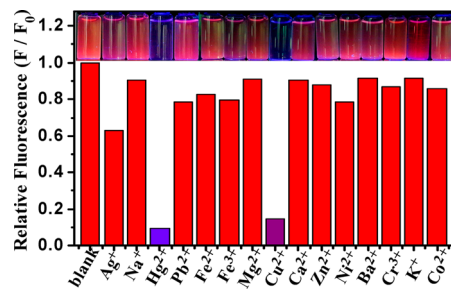


Figure 3. Fluorescence intensity changes of Au-AgNCs (0.417 mM) in the presence of different metal ions of 1.0 μM (insert: photographs under UV light), where F_0 and F correspond to the fluorescence intensity of Au-AgNCs in the absence and presence of metal ions, respectively.

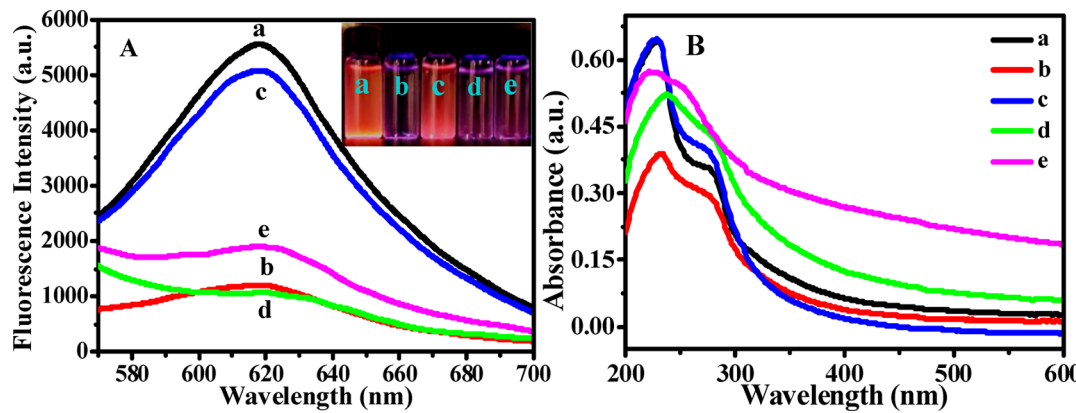


Figure 4. (A) Fluorescence spectra and (B) UV-vis spectra of Au-AgNCs (0.417 mM) in the (a) absence and (b) presence of Cu^{2+} ions, (c) Cu^{2+} ions with EDTA, (d) Hg^{2+} ions, and (e) Hg^{2+} ions with EDTA (insert: photographs under UV light), where $0.6 \mu\text{M}$ Cu^{2+} or Hg^{2+} ions and $1.0 \mu\text{M}$ EDTA were used.

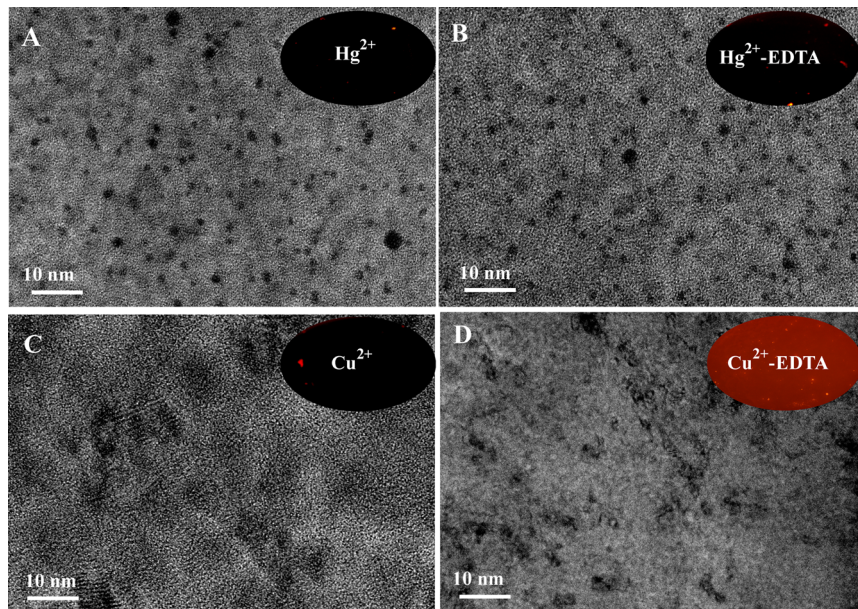


Figure 5. TEM images and the corresponding fluorescence microscopy photographs (insert) of Au-AgNCs in the presence of (A) Hg^{2+} ions, (B) Hg^{2+} ions with EDTA, (C) Cu^{2+} ions, and (D) Cu^{2+} ions with EDTA, where $0.6 \mu\text{M}$ Cu^{2+} or Hg^{2+} ions and $1.0 \mu\text{M}$ EDTA were used.

shows that EDTA might exert a deaggregative effect on the resulting mixture so as to restore the fluorescence of Au-AgNCs, as verified by the corresponding photographs from fluorescence microscopy (insert).

On the basis of the above findings, the quenching mechanism or interaction procedure of bimetallic Au-AgNCs separately with Hg^{2+} and Cu^{2+} ions are thereby proposed. With respect to Hg^{2+} ions, the fluorescence quenching of Au-AgNCs was speculated to result from the interactions between Hg^{2+} ions and Au of Au-AgNCs by metallophilic bonding of their 5d^{10} centers.^{22,31} Such a Hg^{2+} -induced fluorescence quenching of alloying Au-AgNCs is quite different from that by the metallophilic Ag– Hg^{2+} interaction reported previously for the core–shell Au/AgNCs.³⁰ As for Cu^{2+} ions, the fluorescence quenching was thought to result from the synergistic effects of two mixed factors. On the one hand, Cu^{2+} ions might interact with histidyl and carboxyl groups of the protein scaffold of Au-AgNCs to produce a protein– Cu^{2+} complex.³⁴ A protein–protein cross-linking induced by Cu^{2+} ions might thus occur to cause the aggregation of the protein scaffold with Au-AgNCs

toward the fluorescence quenching of Au-AgNCs. On the other hand, the amino acid residues (e.g., tryptophan and tyrosine) of the protein scaffolds could reduce Cu^{2+} to Cu^+ ions,³⁵ which would interact with Ag^+ ions around AgNCs via the metallophilic actions of $3\text{d}^{10}(\text{Cu}^+) \text{--} 4\text{d}^{10}(\text{Ag}^+)$, leading to the fluorescence quenching.^{22,36} Moreover, EDTA as a ligand can chelate with Cu^{2+} ions at a 1:1 ratio and has an affinity higher than that of the protein– Cu^{2+} complex.³⁷ As a result, the introduction of EDTA to the Cu^{2+} -treated Au-AgNCs could cause the deaggregation of the protein– Cu^{2+} complex to restore the lost fluorescence of Au-AgNCs. In regard to Au-AgNCs with Hg^{2+} ions, the lost fluorescence might not be recovered by EDTA because of the formation of strong metallophilic Au– Hg^{2+} bonding aforementioned, although the Hg^{2+} –EDTA chelation is stronger than that of Cu^{2+} –EDTA ($\lg K_{\text{Cu-EDTA}} = 18.8$, $\lg K_{\text{Hg-EDTA}} = 21.5$).³⁰ Therefore, the introduction of the “silver effect” could endow the Au-AgNCs probes the specific ability for sensing Cu^{2+} ions in addition to the enhancement of their red fluorescence. Au-AgNCs-based fluorimetric analysis can thus be expected for Hg^{2+} and Cu^{2+} ions.

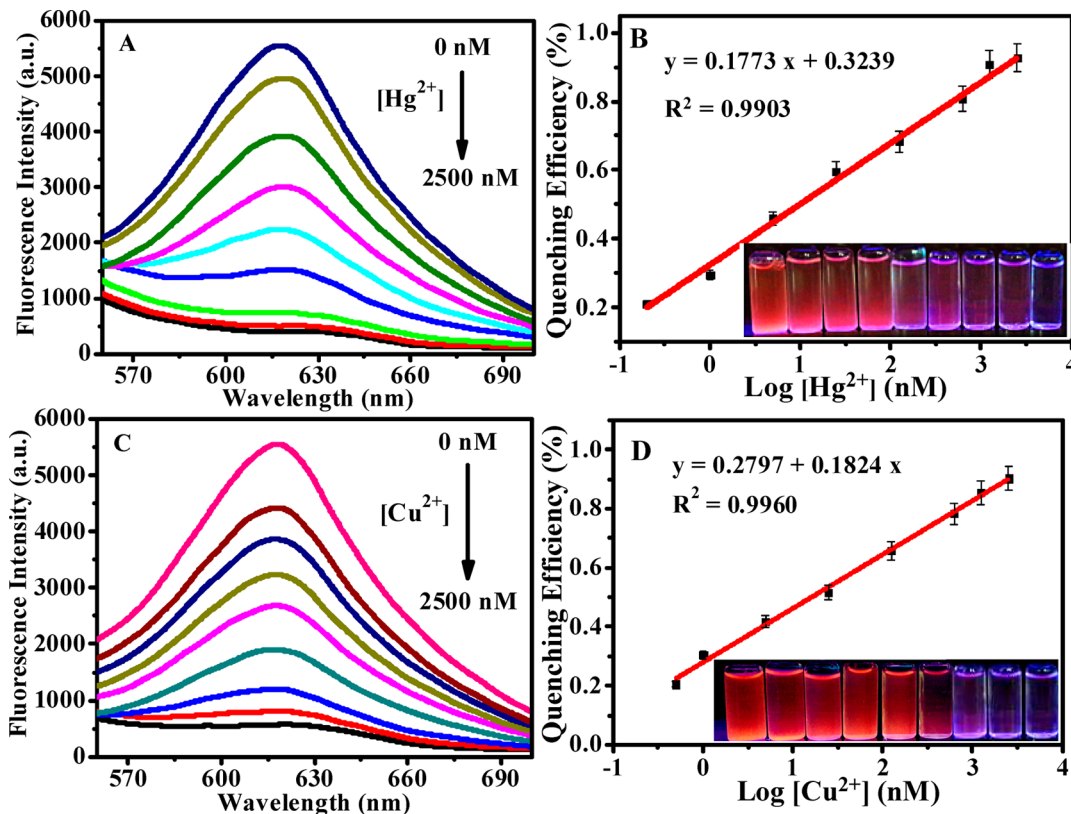


Figure 6. Fluorescence spectra of Au-AgNCs (0.417 mM) upon the addition of (A) Hg^{2+} ions (0, 0.20, 1.0, 5.0, 25, 125, 625, 1250, 2500 nM) and (C) Cu^{2+} ions (0, 0.5, 1.0, 5.0, 25, 125, 625, 1250, 2500 nM) at λ_{ex} 370 nm, corresponding to fluorescence quenching efficiencies versus the logarithmic concentrations of (B) Hg^{2+} ions and (D) Cu^{2+} ions in water (insert: photographs under UV light).

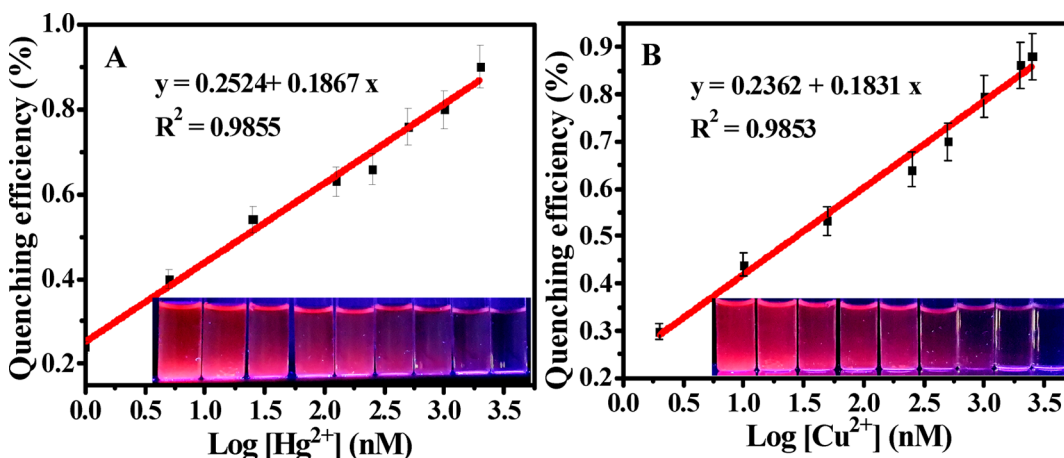


Figure 7. Fluorescence quenching efficiencies of Au-AgNCs (0.417 mM) versus the logarithmic concentrations of (A) Hg^{2+} ions (1.0, 5.0, 25, 125, 250, 500, 1000, 2000 nM) and (B) Cu^{2+} ions (2.0, 10, 50, 250, 500, 1000, 2000, 2500 nM) separately spiked in blood samples (insert: photographs under UV light).

Calibration Curves for Selectively Sensing Hg^{2+} and/or Cu^{2+} Ions. The fluorimetric sensing conditions were first optimized as 0.417 mM Au-AgNCs, pH 7.4, reaction time of 3 min, and 0.60 μM EDTA for Cu^{2+} masking (Figure S6, Supporting Information). The discussion is detailed in Supporting Information.

Under optimal conditions, the developed fluorimetric method was applied for the separate detections of Hg^{2+} and Cu^{2+} ions (Figure 6). Figure 6A manifests the fluorescent spectra of Au-AgNCs with Hg^{2+} ions at different concentrations. The fluorescence intensities decreased gradually as

Hg^{2+} concentrations increased, as also exhibited in the photographs of the corresponding products (Figure 6B, insert). Figure 6B describes the relationship between the logarithms of Hg^{2+} concentrations and fluorescence quenching efficiencies. Accordingly, Hg^{2+} ions can be detected over the linear concentrations ranging from 0.20 to 2500 nM ($R^2 = 0.9903$), with a limit of detection (LOD) of 0.10 nM, estimated by the 3σ rule. Moreover, the fluorescence responses of Au-AgNCs to Cu^{2+} ions at different concentrations were also investigated, with the fluorescent spectra and calibration curve shown in Figure 6, parts C and D, respectively. A good linear relationship

between the quenching efficiencies and the logarithms of the Cu^{2+} concentrations was obtained, ranging from 0.50 nM to 2500 nM ($R^2 = 0.9960$), with an LOD of 0.30 nM.

Furthermore, the developed fluorimetric sensing system was used for the exclusive detection of Hg^{2+} ions coexisting with a high level of Cu^{2+} ions. Figure S7 (Supporting Information) displays the fluorescent responses to Hg^{2+} ions at different concentrations but containing a fixed Cu^{2+} concentration (500 nM), where an aliquot of EDTA was separately added. As shown in Figure S7A, the fluorescent intensities of Au-AgNCs decreased with the increase in Hg^{2+} concentrations. Figure S7B shows a linear correlation obtained for Hg^{2+} ions at concentrations ranging from 0.50 to 3000 nM ($R^2 = 0.9919$). Therefore, the interference from coexisting Cu^{2+} ions could be successfully eliminated in this fluorimetric system, thus allowing for the exclusive detection of Hg^{2+} ions with high sensitivity.

Fluorimetric Analysis of Blood Samples Spiked with Hg^{2+} or Cu^{2+} . The application feasibility of the Au-AgNCs-based fluorimetric method was investigated for blood samples spiked with Hg^{2+} and Cu^{2+} at different concentrations (Figure 7). The relationships between the quenching efficiencies and the logarithms of the concentrations of Hg^{2+} ions (Figure 7A) and Cu^{2+} ions (Figure 7B) were separately obtained. Accordingly, Hg^{2+} ions and Cu^{2+} ions in blood could be quantified in the linear concentration ranges from 1.0 to 2000 nM ($R^2 = 0.9855$) and from 2.0 to 2500 nM ($R^2 = 0.9853$), respectively, corresponding to LODs of 0.30 nM and 0.60 nM. Furthermore, the correlation of the analysis results obtained from the developed fluorimetry method and the classic ICP-MS method in the clinical laboratory was examined by detecting Hg^{2+} and Cu^{2+} ions in real blood samples (Figure S8, Supporting Information). The regression equations for the detection results for Hg^{2+} and Cu^{2+} ions were obtained with correlation coefficients of 0.9826 and 0.9814 ($P > 0.050$), respectively. Obviously, there is no significant difference between the results obtained from the two methods for analyzing Hg^{2+} and Cu^{2+} ions in blood. In addition, the stability of Au-AgNCs stored in the fresh blood was investigated (Figure S9, Supporting Information), showing no significant change of fluorescent intensity up to 7 days. Therefore, the developed fluorimetric strategy with Au-AgNCs as the fluorescent probes promises the potential of serving as a rapid and reliable candidate for the selective and sensitive detection of Hg^{2+} and Cu^{2+} ions, where Au-AgNCs probes with strong red fluorescence might circumvent the problems of interference from the absorption and scattering effects of protein backgrounds in blood.

CONCLUSIONS

In summary, the “silver effect”, which has been recognized to enhance gold catalysis, presents only a small increase in the gold fluorescence of bimetallic core–shell Au@AgNCs prepared by the common two-step biomimetic route. Here, bimetallic alloying Au-AgNCs were successfully synthesized alternatively by using a new facile one-pot biomimetic route via adjusting the molar ratios of Au/Ag precursors in the protein matrix. Dramatically enhanced red fluorescence was unexpectedly obtained for the alloying Au-AgNCs prepared at the vital molar ratio of Au/Ag precursors (i.e., 25/6), compared to that for AuNCs and core–shell Au@AgNCs. More importantly, when the alloying Au-AgNCs were employed to probe 15 kinds of common metal ions, only Hg^{2+} and Cu^{2+} ions could share a significant quenching in the fluorescence of Au-

AgNCs. Herein, the silver component could endow the Au-AgNCs probes the new ability to specifically sense Cu^{2+} ions as well as enhance the response to Hg^{2+} ions. The interaction mechanism and sensing performances of Au-AgNCs involved were systematically characterized by TEM imaging, UV-vis spectra, fluorescence spectra, and fluorescence microscopy. With the unique “silver effect”, bimetallic Au-AgNCs were thereby tailored for a fluorescence quenching-based analysis method for separately probing Hg^{2+} and Cu^{2+} ions in blood. Moreover, use of an efficient Cu^{2+} chelating agent to mask Cu^{2+} ions could facilitate the exclusive detection of Hg^{2+} ions coexisting with a high level of Cu^{2+} ions. Also, reversible Cu^{2+} analysis can be expected by restoring the fluorescence of alloying Au-AgNCs after the tests. In addition, the strong red fluorescence of Au-AgNCs probes could ensure fluorimetric analysis with minimal interference from the protein backgrounds in blood. The developed Au-AgNCs-based fluorimetric strategy is simple, rapid, selective, and highly sensitive, holding great promise for the selective detections of Hg^{2+} and Cu^{2+} ions in the clinical, food hygiene, and environmental monitoring fields. Such a facile and efficient synthesis route may also open a new door toward the preparation of various bimetallic nanoclusters or quantum dots with strong fluorescence. Investigation of the detailed mechanism for forming bimetallic alloying Au-AgNCs with “silver effect”-enhanced fluorescence is in progress in our laboratory.

ASSOCIATED CONTENT

Supporting Information

Reagents and apparatus, results and discussion (optimization of the fluorimetric conditions), structure and composition characterizations (DLS, EDS, XRD, XPS) and optical measurements (composition-dependent fluorescence and UV-vis spectra) of Au-AgNCs, fluorimetric analysis for Hg^{2+} ions with a high level of Cu^{2+} ions, the correlation of analytical results between detection methods for Hg^{2+} and Cu^{2+} ions in blood samples, and stability investigation of Au-AgNCs. This material is available free of charge via the Internet at <http://pubs.acs.org>.

AUTHOR INFORMATION

Corresponding Author

*Tel: +86 537 4456306. Fax: +86 537 4456306. E-mail: huawangqfnu@126.com.

Notes

The authors declare no competing financial interests.

ACKNOWLEDGMENTS

This work is supported by the National Natural Science Foundations of China (no. 21375075) and the Taishan Scholar Foundation of Shandong Province, P. R. China.

REFERENCES

- (1) Fu, X.; Lou, T.; Chen, Z.; Lin, M.; Feng, W.; Chen, L. *ACS Appl. Mater. Interfaces* **2012**, *4*, 1080–1086.
- (2) Guo, C.; Irudayaraj, J. *Anal. Chem.* **2011**, *83*, 2883–2889.
- (3) Uauy, R.; Olivares, M.; Gonzalez, M. *Am. J. Clin. Nutr.* **1998**, *67*, 952S–959S.
- (4) Letelier, M. E.; Lepe, A. M.; Faúndez, M.; Salazar, J.; Marín, R.; Aracena, P.; Speisky, H. *Chem. Biol. Interact.* **2005**, *151*, 71–82.
- (5) Gaetke, L. M.; Chow, C. K. *Toxicology* **2003**, *189*, 147–163.
- (6) Mathur, R.; Balaram, V.; Babu, S. S. *Indian J. Chem., Sect. A* **2005**, *44*, 1619.

- (7) Wu, J.; Boyle, E. A. *Anal. Chem.* **1997**, *69*, 2464–2470.
- (8) Zhu, Z.; Su, Y.; Li, J.; Li, D.; Zhang, J.; Song, S.; Zhao, Y.; Li, G.; Fan, C. *Anal. Chem.* **2009**, *81*, 7660–7666.
- (9) Liu, D.; Qu, W.; Chen, W.; Zhang, W.; Wang, Z.; Jiang, X. *Anal. Chem.* **2010**, *82*, 9606–9610.
- (10) Sun, Z.; Zhang, N.; Si, Y.; Li, S.; Wen, J.; Zhu, X.; Wang, H. *Chem. Commun.* **2014**, *50*, 9196–9199.
- (11) Liu, M.; Zhao, H.; Chen, S.; Yu, H.; Zhang, Y.; Quan, X. *Chem. Commun.* **2011**, *47*, 7749–7751.
- (12) Klein, G.; Kaufmann, D.; Schürch, S.; Reymond, J. L. *Chem. Commun.* **2001**, *561*–562.
- (13) Boiocchi, M.; Fabbrizzi, L.; Licchelli, M.; Sacchi, D.; Vázquez, M.; Zampa, C. *Chem. Commun.* **2003**, 1812–1813.
- (14) Chan, Y.-H.; Chen, J.; Liu, Q.; Wark, S. E.; Son, D. H.; Batteas, J. D. *Anal. Chem.* **2010**, *82*, 3671–3678.
- (15) Koneswaran, M.; Narayanaswamy, R. *Sens. Actuators, B* **2009**, *139*, 91–96.
- (16) Li, J.; Zhu, J. J.; Xu, K. *TrAC, Trends Anal. Chem.* **2014**, *58*, 90–98.
- (17) Xie, J.; Zheng, Y.; Ying, J. Y. *J. Am. Chem. Soc.* **2009**, *131*, 888–889.
- (18) Su, Y. T.; Lan, G.-Y.; Chen, W. Y.; Chang, H. T. *Anal. Chem.* **2010**, *82*, 8566–8572.
- (19) Yu, J.; Choi, S.; Dickson, R. M. *Angew. Chem.* **2009**, *121*, 324–326.
- (20) Retnakumari, A.; Setua, S.; Menon, D.; Ravindran, P.; Muhammed, H.; Pradeep, T.; Nair, S.; Koyakutty, M. *Nanotechnology* **2010**, *21*, 055103_1–12.
- (21) Yoon, B.; Häkkinen, H.; Landman, U.; Wörz, A. S.; Antonietti, J.-M.; Abbet, S.; Judai, K.; Heiz, U. *Science* **2005**, *307*, 403–407.
- (22) Xie, J.; Zheng, Y.; Ying, J. Y. *Chem. Commun.* **2010**, *46*, 961–963.
- (23) Liu, H.; Zhang, X.; Wu, X.; Jiang, L.; Burda, C.; Zhu, J. *J. Chem. Commun.* **2011**, *47*, 4237–4239.
- (24) Hostetler, M. J.; Zhong, C. J.; Yen, B. K.; Anderegg, J.; Gross, S. M.; Evans, N. D.; Porter, M.; Murray, R. W. *J. Am. Chem. Soc.* **1998**, *120*, 9396–9397.
- (25) Ferrando, R.; Jellinek, J.; Johnston, R. L. *Chem. Rev.* **2008**, *108*, 845–910.
- (26) Wang, D.; Cai, R.; Sharma, S.; Jirak, J.; Thummanapelli, S. K.; Akhmedov, N. G.; Zhang, H.; Liu, X.; Petersen, J. L.; Shi, X. *J. Am. Chem. Soc.* **2012**, *134*, 9012–9019.
- (27) Zhou, T. Y.; Lin, L. P.; Rong, M. C.; Jiang, Y. C.; Chen, X. *Anal. Chem.* **2013**, *85*, 9839–9844.
- (28) Sun, J.; Wu, H.; Jin, Y. *Nanoscale* **2014**, *6*, 5449–5457.
- (29) Gui, R.; Wang, Y.; Sun, J. *Microchim. Acta* **2014**, *181*, 1231–1238.
- (30) Pal, T.; Ganguly, M.; Mondal, C.; Pal, J.; Pal, A.; Negishi, Y. *Dalton Trans.* **2014**, *43*, 11557–11565.
- (31) Burini, A.; Fackler, J. P.; Galassi, R.; Grant, T. A.; Omary, M. A.; Rawashdeh-Omary, M. A.; Pietroni, B. R.; Staples, R. J. *J. Am. Chem. Soc.* **2000**, *122*, 11264–11265.
- (32) Gui, R.; Jin, H. *Analyst* **2013**, *138*, 7197–7205.
- (33) Chen, D. H.; Chen, C. J. *J. Mater. Chem.* **2002**, *12*, 1557–1562.
- (34) Løvstad, R. A. *BioMetals* **2004**, *17*, 111–113.
- (35) Wiechelman, K. J.; Braun, R. D.; Fitzpatrick, J. D. *Anal. Biochem.* **1988**, *175*, 231–237.
- (36) Zhang, J. P.; Wang, Y. B.; Huang, X. C.; Lin, Y. Y.; Chen, X. M. *Chem.—Eur. J.* **2005**, *11*, 552–561.
- (37) Muhammed, M. H.; Verma, P. K.; Pal, S. K.; Retnakumari, A.; Koyakutty, M.; Nair, S.; Pradeep, T. *Chem.—Eur. J.* **2010**, *16*, 10103–10112.